

## A WALL-WAKE MODEL FOR TURBULENT BOUNDARY LAYERS WITH PRESSURE GRADIENTS<sup>1</sup>

Ivan Marusic and A. E. Perry

Department of Mechanical and Manufacturing Engineering  
The University of Melbourne  
Parkville, Victoria 3052  
AUSTRALIA

### ABSTRACT

The attached eddy hypothesis is considered here for boundary layers with arbitrary streamwise pressure gradients. It is found that in order to obtain the correct quantitative results for all components of the Reynolds stresses, two basic types of eddy structure geometries are required. The first type, called type-A, is interpreted to give a "wall structure" and the second referred to as type-B gives a "wake structure". This is in analogy with the conventional mean velocity formulation of Coles where the velocity is decomposed into a law of the wall and a law of the wake. If the above mean velocity formulation is accepted then in principle, once the eddy geometries are fixed for the two eddy types, all Reynolds stresses and associated spectra contributed from the attached eddies can be computed without any further empirical constants.

### INTRODUCTION

This paper describes extensions to the work on the attached eddy hypothesis of Townsend (1976) and the model based on this developed at Melbourne by Perry and various co-workers. In most past work the eddies in the attached eddy hypothesis were used only notionally to illustrate functional forms and trends and to aid in dimensional arguments. No serious attempt to produce quantitative results has been made. To do this would require a knowledge of precise eddy shapes. In this paper some tentative shapes are tried and quantitative comparisons are made with data. Although precise shapes for representative eddies are not known and probably will never be known, the authors are convinced that definite conclusions can be drawn concerning important gross properties of the

attached eddy shapes.

The important departures in thinking about the attached eddy hypothesis developed here stems from attempting to describe quantitatively all stress components and associated spectra for boundary layers with streamwise pressure gradients. It is only recently that such data has become available and it is presented here for comparison.

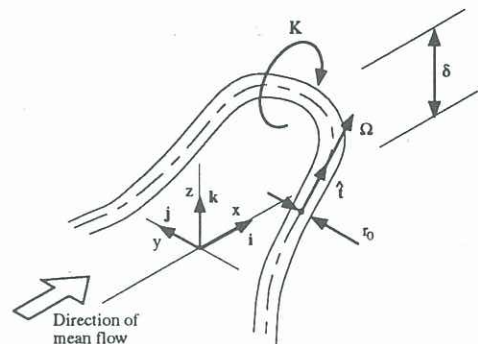


Figure 1: Sketch of a representative attached eddy.

By the term attached eddies we mean a set of geometrically similar eddies consisting of a range of length scales with individual length scales proportional to the distance at which the eddy is located from, or extends above, the wall. The essential finding here is that there are two types of attached eddies which are responsible for most of the turbulent kinetic energy and Reynolds shear stresses. These will be referred to as type-A and type-B eddies. In all previous work only type-A eddies were used in the modelling. See Perry & Marusic (1995) and Marusic & Perry (1995) for a complete describe of the limitations of using type-A eddies alone. Figure 1 shows schematically a representative type-A attached eddy and defines the co-ordinate system to be used in this paper.

<sup>1</sup>A more complete version of this work will appear in Perry & Marusic (1995) and Marusic & Perry (1995).

For type-A eddies, the vortex lines extend to the wall while for type-B the vortex lines undulate in the spanwise direction but do not reach the boundary. It is tentatively proposed here that the type-A eddies are responsible for a universal wall structure and for the mean-flow logarithmic law of the wall, which here extends throughout the layer, whereas type-B structures produce a wake structure (which contributes to "non-universal" turbulence intensities in the wall region) and are responsible for the mean flow wake component. This is consistent with the ideas expressed by Coles (1956,1957) who was concerned only with mean velocities. The wall structure is identical to the "pure wall" flow which occurs in equilibrium sink flow where the Coles wake factor,  $\Pi$  is zero. Figure 2 shows a schematic summary of this two part model. From this hopefully a unified theory can be constructed, valid for favourable, zero and adverse pressure gradient flows.

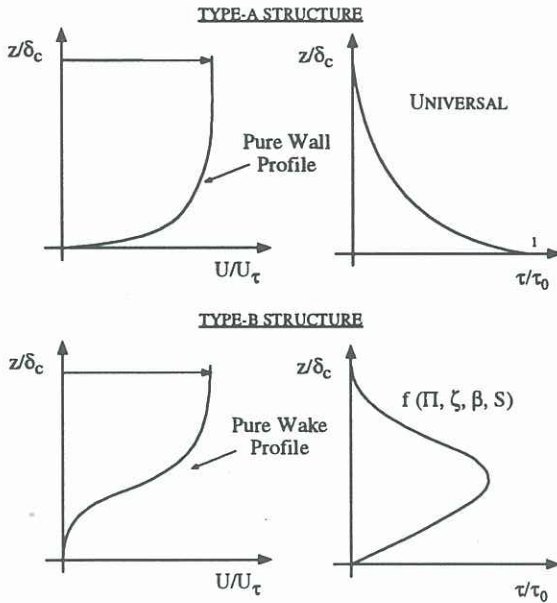


Figure 2: Two part model.

### MODEL FORMULATION

Once the representative eddy shapes for type-A and type-B have been chosen, a calculation of the cross-stream vorticity function,  $f[z/\delta]$ , the eddy intensity functions,  $I_{ij}[z/\delta]$ , and the eddy spectral functions,  $G_{ij}[k_1 z, z/\delta]$  can be made for each eddy. These are functions of eddy geometry alone and are obtained from Biot-Savart law calculated velocity signatures. See Perry & Marusic (1995) for details on calculating these terms.

Estimates of the gradient of mean flow, Reynolds stresses and spectra are obtained by firstly considering arrays of randomly distributed representative eddies distributed over the surface with an average density proportional to  $1/\delta^2$ . The contributions are considered from a range of scales ranging from the

smallest length scale  $\delta_1 = O(100zU_\tau/\nu)$  to  $\delta_c$ , the boundary layer thickness. A probability density function for eddy length scales  $\delta$  is included with the function  $Q[\delta/\delta_c]$  which indicates the deviation from an -1 power law p.d.f. A further weighting function  $T[\delta/\delta_c]$  is also included to account for velocity scale variations between the arrays or hierarchies of different length scales. This results in the following integrals

$$\frac{dU/U_\tau}{dz} = \int_{\delta_1}^{\delta_c} f\left[\frac{z}{\delta}\right] Q\left[\frac{\delta}{\delta_c}\right] D\left[\frac{\delta}{\delta_c}\right] \frac{1}{\delta^2} d\delta,$$

$$\frac{\overline{u_i u_j}}{U_\tau^2} = \int_{\delta_1}^{\delta_c} I_{ij}\left[\frac{z}{\delta}\right] Q^2\left[\frac{\delta}{\delta_c}\right] D\left[\frac{\delta}{\delta_c}\right] \frac{1}{\delta} d\delta,$$

$$\frac{\Phi_{ij}[k_1 z]}{U_\tau^2} = \int_{\delta_1}^{\delta_c} G_{ij}[k_1 z, \frac{z}{\delta}] Q^2\left[\frac{\delta}{\delta_c}\right] D\left[\frac{\delta}{\delta_c}\right] \frac{1}{\delta} d\delta.$$

Here  $U$  is the mean streamwise velocity,  $U_\tau$  is the wall shear velocity and  $\Phi_{ij}[k_1 z]$  is the spectra for the Reynolds stress  $\overline{u_i u_j}$  per non-dimensional wavenumber  $k_1 z$ . By using the logarithmic variables:  $\lambda = \log[\delta/z]$ ,  $\lambda_E = \log[\delta_c/z]$  and  $\lambda_1 = \log[\delta_1/z]$  the above equation are transformed into the following convolution equations

$$\frac{dU_D^*}{d\lambda_E} = \int_{-\infty}^{\infty} h[\lambda] e^{-\lambda} T[\lambda - \lambda_E] w[\lambda - \lambda_E] d\lambda,$$

$$\frac{\overline{u_i u_j}}{U_\tau^2} = \int_{-\infty}^{\infty} J_{ij}[\lambda] T^2[\lambda - \lambda_E] w[\lambda - \lambda_E] d\lambda,$$

$$\frac{\Psi_{ij}[\alpha_z]}{U_\tau^2} = \int_{-\infty}^{\infty} g_{ij}[\alpha_z, \lambda] T^2[\lambda - \lambda_E] w[\lambda - \lambda_E] d\lambda,$$

where  $U_D^* = (U_1 - U)/U_\tau$ ,  $U_1$  is the freestream velocity,  $w[\lambda - \lambda_E] = D[\delta/\delta_c]$ ,  $T[\lambda - \lambda_E] = Q[\delta/\delta_c]$ ,  $h[\lambda] = f[z/\delta]$ ,  $J_{ij}[\lambda] = I_{ij}[z/\delta]$ ,  $g_{ij}[\alpha_z, \lambda] = k_1 z G_{ij}[k_1 z, z/\delta]$ ,  $\Psi_{ij}[\alpha_z] = k_1 z \Phi_{ij}[k_1 z]$ , and  $\alpha_z = \log[k_1 z]$ . The functions  $w$  and  $T$  switch to zero when  $\lambda < \lambda_1$  and  $\lambda > \lambda_E$ . This effectively controls the limits of the integration.

The contributions from the type-A and type-B structures simply add together to form the final composite result, i.e.

$$\frac{dU_D^*}{d\lambda_E} = \left(\frac{dU_D^*}{d\lambda_E}\right)_A + \left(\frac{dU_D^*}{d\lambda_E}\right)_B, \quad (1)$$

$$\frac{\overline{u_i u_j}}{U_\tau^2} = \left(\frac{\overline{u_i u_j}}{U_\tau^2}\right)_A + \left(\frac{\overline{u_i u_j}}{U_\tau^2}\right)_B, \quad (2)$$

$$\frac{\Psi_{ij}[\alpha_z]}{U_\tau^2} = \left(\frac{\Psi_{ij}[\alpha_z]}{U_\tau^2}\right)_A + \left(\frac{\Psi_{ij}[\alpha_z]}{U_\tau^2}\right)_B. \quad (3)$$

### Shear stress distribution

In order to develop the model further, analytical expressions for the shear stress distribution are used. Such an expression is given by Perry, Marusic & Li (1994) in the form

$$\frac{\tau}{\tau_0} = f_1[\eta, \Pi, S] + g_1[\eta, \Pi, S]\zeta + g_2[\eta, \Pi, S]\beta \quad (4)$$



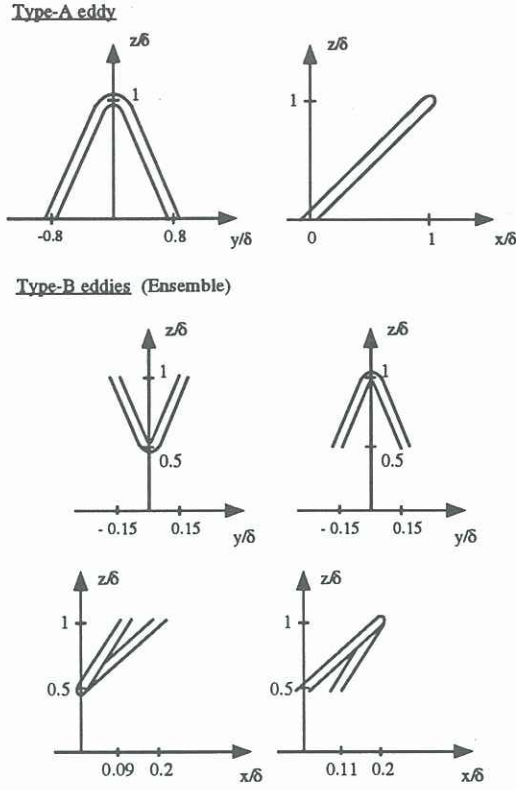


Figure 3: Type-A and type-B eddy structures chosen for calculation. The type-B structure is an ensemble of the above with their corresponding "reflections" in the  $x - z$  plane (not shown here).  $\tau_0/\delta = 0.05$  in all cases; Gaussian distribution of vorticity is assumed in the vortex tubes.

where  $\eta = z/\delta_c$ ,  $\tau_0$  is the wall shear stress,  $\Pi$  is the Coles wake factor,  $S = U_1/U_\tau$ ,  $\zeta = S\delta_c d\Pi/dx$ , and  $\beta = (\delta^*/\tau_0)(dP/dx)$ . All of these terms are obtained from the mean flow. Equation (4) was derived by using Coles (1956) law of the wall and wake together with the two-dimensional mean streamwise momentum and continuity equations. As shown in figure 2, the distribution for shear stress is assumed to be universal for the "wall structure" (case  $\Pi = 0$ ). This is equivalent to universal "sink" flow and (4) reduces to

$$\left(\frac{\tau}{\tau_0}\right)_A = 1 - \eta + \eta \log[\eta]. \quad (5)$$

### COMPARISON OF MODEL WITH EXPERIMENT

The model is used here to calculate the Reynolds stresses and spectra given the mean flow conditions  $\Pi$ ,  $S$ ,  $\zeta$  and  $\beta$ . Once these parameters are provided and once the eddy shapes have been chosen (thus giving  $J_{ij}$  and  $g_{ij}$ ) equations (4) and (5) and (2) are used to solve  $(T^2w)_A$  and  $(T^2w)_B$  using a deconvolution procedure. Once these have been solved, they are substituted back into equations (2) and (3) to solve for the remaining Reynolds stresses and spectra.

Figure 4 shows a comparison of computed Reynolds

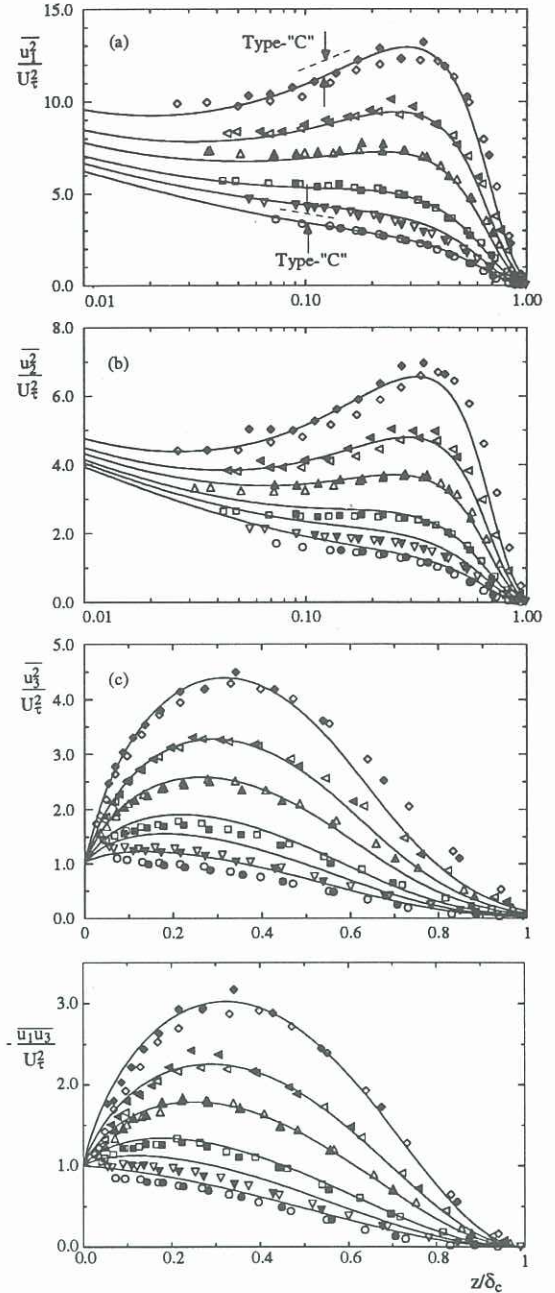


Figure 4: Reynolds stresses (nonequilibrium data - see Table 1) compared to attached eddy formulation using type-A and type-B eddies.

$x(\text{mm})$	$\Pi$	$S$	$\zeta$	$\beta$	$R_\theta$	$K_\tau$
1200	0.42	23.6	0.15	$\approx 0.0$	2206	1028
1800	0.68	25.4	0.94	0.65	3153	1203
2240	1.19	28.1	2.18	1.45	4155	1234
2640	1.87	31.5	4.64	2.90	5395	1265
2880	2.46	34.5	8.01	4.48	6395	1280
3080	3.23	38.40	15.32	7.16	7257	1253

Table 1: Experimental mean flow parameters (Marusic (1991) 10APG flow).  $R_\theta = \theta U_1/\nu$  and  $K_\tau = \delta_c U_\tau/\nu$ .

stresses for the data described in Table 1 using type-A and type-B eddy shapes shown in figure 3. The type-B eddy shapes are an approximation to an span-

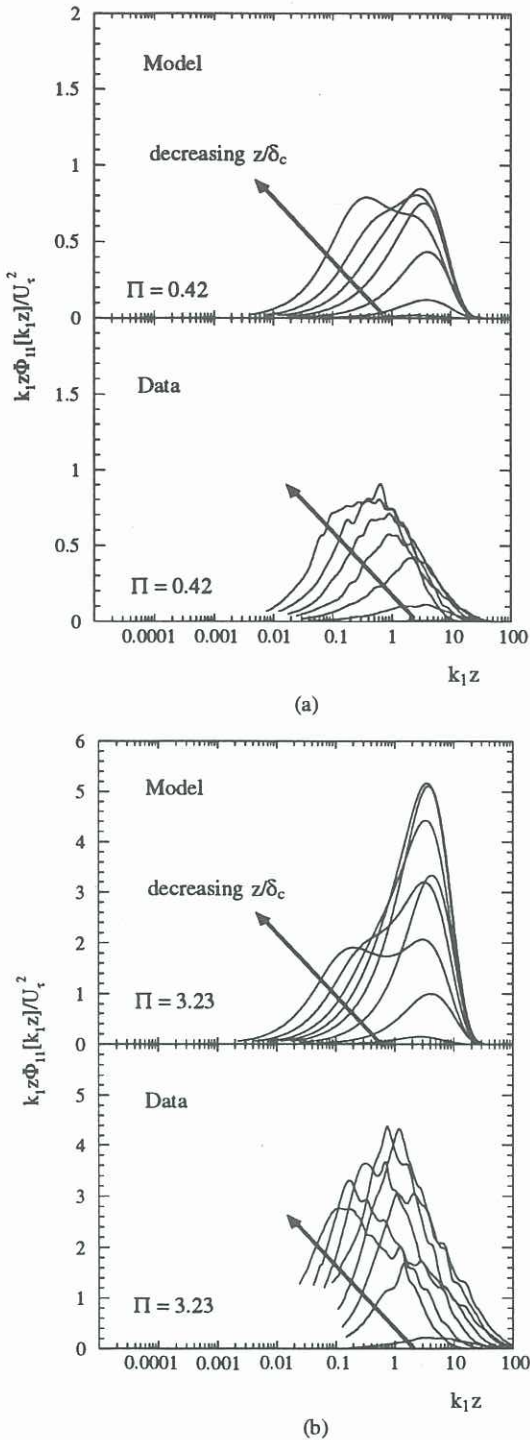


Figure 5: Premultiplied streamwise spectra from model and authors' data. (a)  $\Pi = 0.42$  (10APG) flow case.  $z/\delta_c = 0.10, 0.17, 0.27, 0.39, 0.54, 0.72, 0.93$ . (b)  $\Pi = 3.23$  (10APG) flow case, as in (a) with extra level  $z/\delta_c = 0.05$ .

wise undulating structure. From Table 1, the experimental data is seen to be far from "equilibrium" with  $\zeta = S\delta_c d\Pi/dx$  values increasing with streamwise distance. The experimental results include both stationary (unshaded symbols) and flying hot-wire (shaded symbols) measurements - see Maru-

sic (1991) for further details.

The agreement between the experiment and model is seen to be good. Perry & Marusic (1995) and Marusic & Perry (1995) have compared the model to additional experimental data including equilibrium data flow cases. In all cases agreement with the Reynolds stresses appears to be of good quality. Corresponding spectra are also compared in figure (5). Here, although the model shows excellent qualitative agreement with the data, some quantitative differences are noted. This would suggest that the tentative shapes shown in figure 3 are not quite right. Further refinement of eddy shape would consequently be required in any further studies although it would appear that the gross properties of the representative eddies shown in figure 3 are correct.

An additional unknown which prevents the precise eddy shapes to be known at this stage are the high wavenumber contributions which are missing in this "inviscid" model. Perry, Henbest & Chong (1986) have discussed the role of possible further structures which contribute to the high wavenumber motions. These will be collectively referred to as type-C eddies. These are probably detached eddies, i.e. their length scale is not related directly to the distance they are located from the wall. The eddies in the Kolmogorov inertial subrange and dissipation range form a subset of type-C structures. Tentative empirical estimates of the approximate type-C contributions are indicated on figure 4.

Resolving this high wavenumber discrepancy remains one of the problems yet to be solved for completing the model. However, if closure requires only the connection between velocity defect shapes, Reynolds shear stresses and other quantities associated with low wavenumber phenomena, this may not be an important drawback.

## REFERENCES

- Coles, D.E. (1956). *J. Fluid Mech.* **1**, 191-226.
- Coles, D.E. (1957). *J. Aero. Sci.* **24**, 459-506.
- Marusic, I. (1991) Ph.D. Thesis, Uni. of Melbourne
- Marusic, I. & Perry, A.E (1995) *J. Fluid Mech.* **298**, 389-407.
- Perry, A.E., Henbest S.M. & Chong, M.S. (1986) *J. Fluid Mech.* **165**, 163-199.
- Perry, A.E., Marusic, I., & Li, J.D. (1994). *Phys. Fluids* **2** (6), 1024-1035.
- Perry, A.E. & Marusic, I. (1995) *J. Fluid Mech.* **298**, 361-388.
- Townsend, A.A. (1976) *The structure of turbulent shear flow*. Cambridge Uni. Press.